

# Adaptive DRX Scheme to Improve Energy Efficiency in LTE Networks with Bounded Delay

Sergio Herrería-Alonso, Miguel Rodríguez-Pérez, *Member, IEEE*,  
Manuel Fernández-Veiga, *Senior Member, IEEE*, and Cándido López-García

**Abstract**—The Discontinuous Reception (DRX) mechanism is commonly employed in current LTE networks to improve energy efficiency of user equipment (UE). DRX allows UEs to monitor the physical downlink control channel (PDCCH) discontinuously when there is no downlink traffic for them, thus reducing their energy consumption. However, DRX power savings are achieved at the expense of some increase in packet delay since downlink traffic transmission must be deferred until the UEs resume listening to the PDCCH. In this paper, we present a promising mechanism that reduces energy consumption of UEs using DRX while simultaneously maintaining average packet delay around a desired target. Furthermore, our proposal is able to achieve significant power savings without either increasing signaling overhead or requiring any changes to deployed wireless protocols.

**Index Terms**—Energy efficiency, LTE, LTE-Advanced, DRX

## I. INTRODUCTION

Current generation wireless networks such as Long Term Evolution (LTE) and LTE-Advanced (LTE-A) are able to achieve high data rates up to 1 Gb/s by adopting several advanced modulation, coding and multiple antenna techniques [1]. This great increment on the offered capacity for data transmission has also increased the power demands of mobile devices substantially.

To improve user equipment (UE) battery lifetime, LTE supports Discontinuous Reception (DRX) [2], [3] in both the RRC\_IDLE and the RRC\_CONNECTED radio resource control (RRC) states [4]. DRX allows UEs which are not receiving data from their corresponding eNodeB (eNB) to monitor the physical downlink control channel (PDCCH) discontinuously. When UEs are not listening to the PDCCH, they can enter a power saving mode in which most of their circuits can be turned off, thus reducing power consumption significantly. With DRX, the UE only wakes up periodically to listen to the PDCCH for a while, returning to the low power mode if no packet arrival is detected or resuming its normal operation in the case of new packet arrivals.

Obviously, DRX power savings are achieved at the expense of increasing packet delay since all the traffic for UEs in the low power mode must be buffered at the eNB until they listen to the PDCCH again. Therefore, a careful configuration of the main DRX parameters is critical to maintain a reasonable latency for active traffic while obtaining significant power

savings at the UEs [3], [5]. DRX is configured per UE (as opposed to per radio bearer) and there is only one DRX configuration active in each UE at any time. Unfortunately, a single DRX configuration fails to provide a satisfactory service to any possible user activity level. Thus, several algorithms have been proposed to configure DRX parameters according to the ongoing traffic activity in a way that leads to a good trade-off between power savings and packet delay [3], [6], [7], [8], [9], [10], [11], [12], [13]. All these schemes require, therefore, the reconfiguration of DRX parameters whenever traffic characteristics change substantially. However, DRX reconfiguration is carried out via RRC signaling, so these schemes would cause considerable increments in signaling overhead, especially when the number of UEs using DRX in a given cell is large [14].

In this paper we present a promising mechanism to improve energy efficiency of UEs using DRX that is able to control the average packet delay with any fixed configuration of DRX parameters and, therefore, does not increase signaling overhead. Our proposal is based on the well-known packet coalescing technique successfully applied beforehand to reduce energy consumption in other networking fields such as Ethernet interfaces [15], [16] and EPON systems [17], [18]. With current DRX, an eNB with some downlink traffic queued for a given UE in the low power mode will not send this traffic until the next time the UE monitors the PDCCH. Notice that, as soon as the UE detects a new packet arrival, it abandons DRX mode and returns to normal operation. Therefore, the amount of time that UEs spend in the low power mode can be easily increased if the eNB just delays packet transmission to those UEs in DRX mode until their corresponding downstream queues reach a certain threshold. However, a single threshold value does not suit well for any possible downlink traffic, so our proposal includes an adaptive algorithm able to adjust this parameter to real time traffic characteristics with the goal of maintaining average packet delay around a given target while keeping energy consumption low enough.

In addition, our proposal is very simple to setup since it only requires configuring two straightforward parameters: the average and the maximum queueing delay desired for packets at the eNB. Furthermore, the algorithm can be easily deployed in current LTE/LTE-A networks since it only demands some minor changes to the operations of the eNB, keeping existent wireless protocols unmodified.

The rest of this paper is organized as follows. Section II presents the basic operations of DRX and Section III describes the proposed scheme. We refer to our proposal as coalesced

The authors are with the Telematics Engineering Dept., Univ. of Vigo, 36310 Vigo, Spain. Tel.: +34 986 813458; fax: +34 986 812116; email: sha@det.uvigo.es (S. Herrería-Alonso).

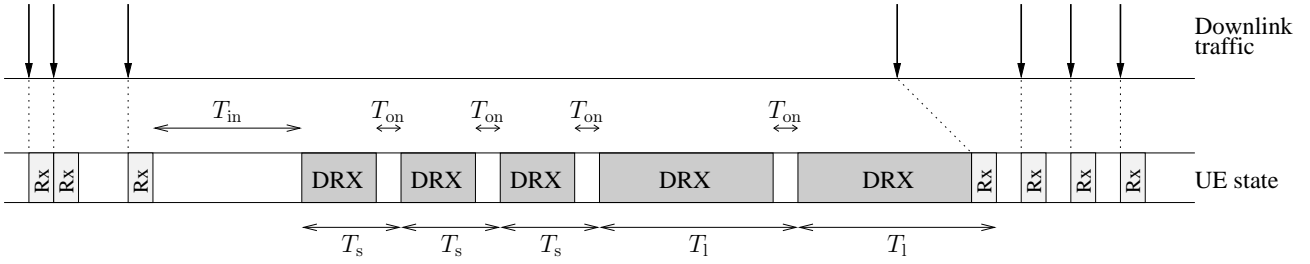


Fig. 1. DRX operations with  $N_s = 3$ .

DRX. In Section IV we develop an analytic model to compute the average packet delay introduced by coalesced DRX. We next particularize this model to Poisson traffic in Section V. This model is used in Section VI to devise an adaptive algorithm able to adjust the queue threshold used in coalesced DRX according to traffic conditions. Section VII shows some results obtained through simulation. In Section VIII we discuss some implementation issues and compare our proposal with previous work in this field. Finally, the main conclusions are summarized in Section IX.

## II. DRX OPERATIONS

The DRX mechanism is frequently used in LTE/LTE-A networks to reduce the power consumption of mobile handsets. Although this mechanism can be configured in both the RRC\_IDLE and the RRC\_CONNECTED states, we assume that UEs are always in the latter state, as it is the usual case for those UEs with multiple applications running in the background [19].

In the RRC\_CONNECTED state, a two-level power-saving scheme with both short and long DRX cycles is used. Figure 1 depicts a typical example of the main DRX operations. When DRX is enabled, UEs stop listening to the PDCCH and enter a low power mode. While in this sleeping mode, UEs cannot receive packets, so the eNB must delay the transmission of all their downlink traffic until they monitor the PDCCH again. Then, sleeping UEs periodically wake up to listen to the PDCCH for a short interval to check for new packet arrivals.

DRX configuration involves setting various parameters during the radio bearer establishment. The DRX parameters considered in this paper are:

- Inactivity timer ( $T_{in}$ ): time to wait before enabling DRX. This timer is immediately re-initiated after a successful reception on the PDCCH. When this timer expires, the UE enables DRX and enters the short DRX cycle.
- Short DRX cycle ( $T_s$ ): duration of the first DRX cycles after enabling DRX.
- DRX short cycle timer ( $N_s$ ): long DRX cycles will be applied after this timer expires. It is usually expressed as the number of short DRX cycles before transitioning to long DRX cycles.
- Long DRX cycle ( $T_1$ ): duration of DRX cycles after  $N_s$  short DRX cycles ( $T_1 \geq T_s$ ).
- On-duration timer ( $T_{on}$ ): interval at every DRX cycle during which the UE monitors the PDCCH checking for the arrival of a new packet ( $T_{on} \ll T_s$ ). A successful

reception on the PDCCH during this interval finishes the DRX cycle immediately and the inactivity timer is started again.

We also assume that the LTE network is lightly loaded and that, therefore, radio resources are always available to the UE when required. It is expected that this will be the most likely scenario in the near future since mobile networks are now rapidly evolving to include small cells (such as picocells and femtocells), thus reducing the number of users competing for resources at each base station [20]. On the other hand, if the network were lightly congested, a DRX-aware scheduling scheme would be required at the eNB to resolve resource contention among UEs. This is out of the scope of our paper, but a scheduler similar to those proposed in [21], [22] that keeps aware of DRX operations and mitigates resource contention could be applied.

## III. COALESCED DRX

As explained in the previous section, an eNB with some downlink traffic queued for a given UE in DRX mode will not send this traffic until the UE monitors the PDCCH again (i.e., in the next on-duration interval). Therefore, the eNB is already carrying out an implicit packet coalescing because a significant period of time may be spanned since it receives a packet for the sleeping UE until the actual beginning of transmission ( $T_1 - T_{on}$  at most). However, note that current eNBs will start downlink delivery even if only a single packet is awaiting transmission.

In this paper we propose that eNBs delay downlink transmission to UEs in DRX mode until their corresponding downstream queues reach a certain tunable threshold ( $Q_w$ ). Figure 2 shows an example of coalesced DRX operations with  $Q_w = 3$  packets.<sup>1</sup> Instead of starting packet transmission as soon as there is new traffic to transmit, the eNB waits until  $Q_w$  packets are accommodated in the downstream queue, thus reducing the number of transitions between the DRX and the active mode and, therefore, increasing the amount of time the UE remains in the low power mode. Note that downlink transmission is delayed even when new packets arrive during on-duration intervals if the  $Q_w$  threshold has not yet been reached. Once the DRX mechanism has been disabled, packets arriving before the inactivity timer expires are transmitted as soon as possible. In short, what our proposal makes in practice

<sup>1</sup>Although the queue threshold is specified in packets for simplicity, in a real setting it should be specified in bytes to handle packets of different sizes.

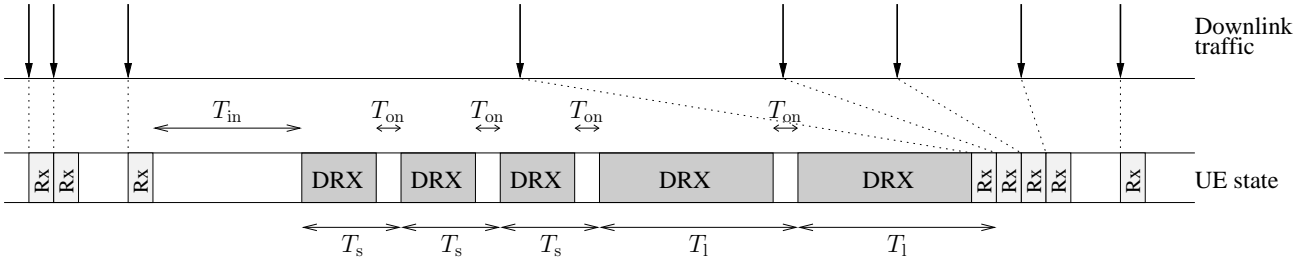


Fig. 2. Coalesced DRX with  $Q_w = 3$  packets.

is just adjusting the duration of DRX cycles, but without the need for performing an actual reconfiguration of DRX parameters.

Obviously, this backlog will provide greater energy savings in the UEs at the expense of increasing packet delay. To avoid delaying downlink traffic excessively, the maximum time  $W_{\max}$  an eNB can delay packet transmission must be bounded.

#### IV. DELAY MODEL

In this section, we will quantify the impact of coalesced DRX on packet delay. Particularly, we compute the average queueing delay,  $E[W]$ , following a similar approach to that used in [23] for queueing systems with vacations in which the first packet in every busy period suffers a random delay  $W_f$  before its transmission begins. For simplicity, we assume that  $T_s = T_1$ , that is, all DRX cycles are of equal length.<sup>2</sup>

Figure 3 illustrates several definitions that will be used in the model. We consider that packet arrivals at the eNB for a given UE follow a general distribution with independent inter-arrival times  $A_n$ ,  $n = 1, 2, \dots$ , and average arrival rate  $\lambda$ . The sequence of service times  $S_n$ ,  $n = 1, 2, \dots$ , demanded by successive packets is a set of random variables with a common, although arbitrary, distribution function and mean service rate  $\mu$ . Obviously, the utilization factor  $\rho = \lambda/\mu$  must be less than 1 to assure system stability. A notation summary is provided in Table I.

##### A. Average Queueing Delay

Let  $O_n$  be the inter-output times, that is, the time between the end of transmissions of  $n$ -th and  $(n+1)$ -th packets. Clearly,

$$O_n = A_n + D_{n+1} - D_n, \quad (1)$$

where  $D_n = W_n + S_n$  is the total time that the  $n$ -th packet spends in the eNB and encompasses the corresponding queueing and service times ( $W_n$  and  $S_n$ , respectively). On the other hand, inter-output times can be also obtained as:

$$O_n = X_n + S_{n+1}, \quad (2)$$

<sup>2</sup>This is the default configuration in actual DRX systems since short DRX cycles are optional and need to be explicitly configured. In any case, considering different long and short DRX cycles would only obfuscate the theoretical analysis without providing further insight into the operations of our proposal since it does not rely on any particular DRX configuration.

where  $X_n$  is the idle time elapsed since the end of the  $n$ -th packet transmission until the beginning of the  $(n+1)$ -th packet transmission, so equating (1) and (2) we get

$$W_{n+1} = X_n + D_n - A_n. \quad (3)$$

Squaring both sides of (3), we have

$$\begin{aligned} W_{n+1}^2 &= X_n(X_n + 2(D_n - A_n)) + (A_n - D_n)^2 \\ &= Y_n + (S_n - A_n)^2 + W_n^2 + 2W_n(S_n - A_n), \end{aligned} \quad (4)$$

where  $Y_n \triangleq X_n(X_n + 2(D_n - A_n))$ . Then, taking expectations and assuming stationarity in the system, it follows that

$$E[W] = \frac{-E[U^2] - E[Y] + 2\sigma(W, A)}{2E[U]}, \quad (5)$$

where  $U_n \triangleq S_n - A_n$  and  $\sigma(W, A) \triangleq \sigma(W_n, A_n)$  for packet  $n$ . Although the subscript  $n$  is suppressed for clarity, it should be kept in mind that  $\sigma(W, A)$  is the covariance between the wait in queue of some packet and the time until the next packet arrives. To calculate  $E[Y] = E[X_n(X_n + 2(D_n - A_n))]$ , we must consider the following three cases:

- Case 1)  $A_n - D_n \leq 0$ : this occurs when a new packet arrives at the eNB while it is transmitting traffic to the UE, so  $X_n = 0$ .
- Case 2)  $0 < A_n - D_n \leq T_{\text{in}}$ : a new packet arrives at the eNB before the inactivity timer expires, so DRX has not yet been enabled and the packet can be immediately transmitted. Therefore,  $X_n = A_n - D_n = I$ , where  $I$  is the length of the empty period in the coalescing cycle, that is, the period with no packets in the downstream queue.
- Case 3)  $A_n - D_n > T_{\text{in}}$ : a new packet arrives at the eNB with DRX active, so it cannot be transmitted until the UE re-listens to the PDCCH during a subsequent on-duration interval. In this case,  $X_n = I + W_f$ , where  $W_f$  is the time that the first arriving packet in the coalescing cycle has to wait before it can be transmitted, that is, the queueing delay experienced by the first coalesced packet.

If we denote by  $p_k$ ,  $k \in \{1, 2, 3\}$ , the probability that a new packet arrives at the eNB under the conditions determined by former case  $k$ , then

$$\begin{aligned} E[Y] &= p_2 E[I(I - 2I)] + p_3 E[(I + W_f)(I + W_f - 2I)] \\ &= p_3 E[W_f^2] - (p_2 + p_3) E[I^2] \\ &= p_3 E[W_f^2] - (1 - p_1) E[I^2]. \end{aligned} \quad (6)$$

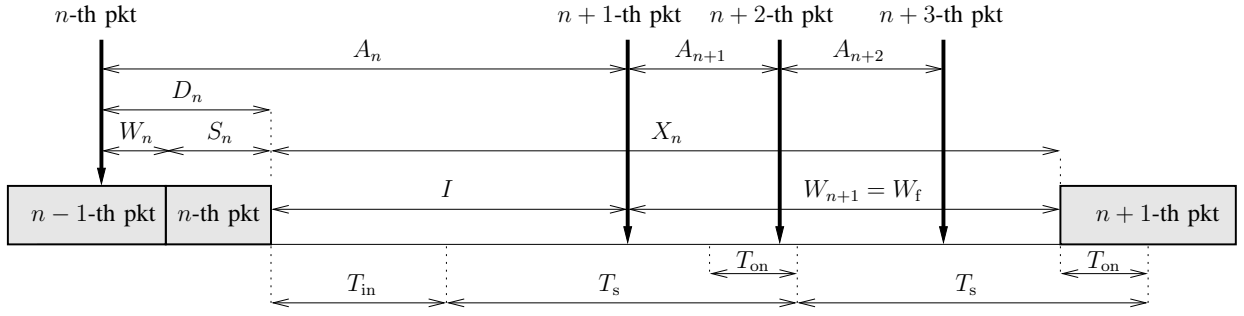


Fig. 3. Coalesced DRX cycle with  $Q_w = 3$  packets.

TABLE I  
NOTATION SUMMARY.

Category	Notation	Description
Traffic characteristics	$A_n$	Time between the arrivals of $n$ -th and $(n+1)$ -th packets
	$S_n$	Service time demanded by $n$ -th packet
	$\lambda$	Average arrival rate
	$\mu$	Average service rate
Model variables	$\rho$	Utilization factor
	$O_n$	Time between the end of transmissions of $n$ -th and $(n+1)$ -th packets
	$D_n$	Total time the $n$ -th packet spends in the eNB
	$W_n$	Queueing delay of the $n$ -th packet
	$X_n$	Idle time since end of $n$ -th packet tx until start of $(n+1)$ -th packet tx
	$Y_n$	$X_n(X_n + 2(D_n - A_n))$
	$U_n$	$S_n - A_n$
	$I$	Length of the empty period in the coalescing cycle
DRX parameters	$W_f$	Queueing delay of the first coalesced packet in the cycle
	$\gamma$	Inverse of the fraction of idle time at the eNB with DRX enabled
	$T_{in}$	Inactivity timer
	$T_{on}$	On-duration timer
	$T_s$	Short DRX cycle duration
	$T_l$	Long DRX cycle duration
Coalesced DRX parameters	$N_s$	DRX short cycle timer
	$Q_w$	Queue threshold
	$Q_{max}$	Maximum queue threshold
	$W^*$	Target average queueing delay
	$W_{max}$	Maximum queueing delay

On the other hand, from (3) we know that

$$X_n = W_{n+1} - D_n + A_n = W_{n+1} - (W_n + S_n) + A_n, \quad (7)$$

so

$$E[X] = E[A] - E[S] = -E[U]. \quad (8)$$

Additionally,  $E[X]$  can be obtained as

$$E[X] = p_2 E[I] + p_3 E[I + W_f] = p_3 E[W_f] + (1 - p_1) E[I]. \quad (9)$$

Therefore, substituting (6), (8) and (9) into (5), and replacing  $(1 - p_1)/p_3$  with  $\gamma$ , we get

$$E[W] = -\frac{E[U^2]}{2E[U]} + \frac{E[W_f^2] - \gamma E[I^2]}{2(E[W_f] + \gamma E[I])} + \frac{\sigma(W, A)}{E[U]}. \quad (10)$$

In the following subsection, we will explain in greater detail the significance of the  $\gamma$  factor introduced. We now calculate the first two moments of variable  $U$  simply as

$$E[U] = E[S - A] = E[S] - E[A] = \frac{1}{\mu} - \frac{1}{\lambda} = -\frac{1 - \rho}{\lambda}, \quad (11)$$

and

$$E[U^2] = \sigma_U^2 + E[U]^2 = \sigma_S^2 + \sigma_A^2 + \left(\frac{1 - \rho}{\lambda}\right)^2, \quad (12)$$

since  $\sigma(S_n, A_n) = 0$  if it is assumed that packet lengths are independent from the arrival process.

Regarding  $\sigma(W, A)$ , note that the waiting time of the first  $Q_w - 1$  packets in each coalescing cycle depends on the inter-arrival times of subsequent packets, so this covariance term must be nonzero. In [24] it is proved that, for single-server queues that wait until  $Q_w$  customers are present before starting service again, this covariance term is given by

$$\sigma(W, A) = \frac{(1 - \rho)(Q_w - 1)\sigma_A^2}{Q_w - 1 + \lambda E[I]}. \quad (13)$$

Finally, substituting (11), (12) and (13) into (10), we get

$$E[W] = \frac{\lambda^2(\sigma_S^2 + \sigma_A^2) + (1 - \rho)^2}{2\lambda(1 - \rho)} + \frac{E[W_f^2] - \gamma E[I^2]}{2(E[W_f] + \gamma E[I])} - \frac{\lambda(Q_w - 1)\sigma_A^2}{Q_w - 1 + \lambda E[I]}. \quad (14)$$

### B. The $\gamma$ Factor

The  $\gamma$  factor introduced in the previous analysis has been defined as the ratio between the probabilities  $1 - p_1$  and  $p_3$ . Recall that  $p_1$  is the probability that a new packet arrives at the eNB while it is transmitting downlink traffic to the UE, so  $1 - p_1$  is the probability that a new packet arrives when the eNB is idle. On the other hand,  $p_3$  is the probability that a new packet arrives when the eNB is idle but it has nevertheless to wait to be served since DRX is active. So,  $\gamma$  is the inverse of the fraction of the idle time at the eNB with DRX enabled.

The probability  $p_1$  can be obtained as

$$p_1 = P[A_n - D_n \leq 0] = P[A_n \leq D_n] = \int_0^\infty F_A(t) f_D(t) dt, \quad (15)$$

where  $F_A(t)$  is the cumulative distribution function of inter-arrival times and  $f_D(t)$  is the probability density function of the total time spent by each packet in the eNB. Similarly, the probability  $p_3$  is directly

$$p_3 = P[A_n - D_n > T_{in}] = 1 - \int_0^\infty F_A(t + T_{in}) f_D(t) dt. \quad (16)$$

Therefore,  $\gamma$  is

$$\gamma = \frac{1 - \int_0^\infty F_A(t) f_D(t) dt}{1 - \int_0^\infty F_A(t + T_{in}) f_D(t) dt} \geq 1. \quad (17)$$

Notice from (14) that the higher this factor is, the lower packet delays we get. For example, if we configure DRX with a high  $T_{in}$  value (a high  $\gamma$  value), the added delay will be reduced since the probability that a packet arrives at the eNB with DRX disabled will be increased and, therefore, it will be more likely transmitted at once. As usual, this reduction in packet latency can only be obtained at the expense of increasing power consumption.

## V. POISSON TRAFFIC

Here we will particularize the previous model for Poisson traffic, that is, assuming that the number of packets that arrive at the eNB in a given interval of time follows a Poisson distribution with average arrival rate  $\lambda$  and variance  $\sigma_A^2 = 1/\lambda^2$ . Although it is well-known that packet arrivals do not generally follow a Poisson distribution, this approximation can be used to model background traffic generated by mobile applications when the UE is in unattended mode [7].

As can be seen from (14), to complete the computation of the average queueing delay, we still have to calculate the average duration of empty periods  $E[I]$  (and  $E[I^2]$ ), the average waiting time of the first packet in each coalescing cycle  $E[W_f]$  (and  $E[W_f^2]$ ), and the  $\gamma$  factor for this particular traffic distribution.

### A. Average Duration of Empty Periods

With Poisson traffic, inter-arrival times are exponentially distributed. Due to the memoryless property of this distribution, the distribution of empty periods is equivalent to that of inter-arrival times, so  $E[I] = 1/\lambda$  and  $E[I^2]$  can be easily calculated as  $E[I^2] = E[A^2] = \sigma_A^2 + E[A]^2 = 2/\lambda^2$ .

### B. Average Waiting Time of the First Packet in Each Cycle

With coalesced DRX, the first arriving packet in each coalescing cycle has to wait for the arrival of other  $Q_w - 1$  packets before the eNB is able to start its transmission, i.e.,  $(Q_w - 1)/\lambda$  on average. Actually, transmission cannot begin until the destination UE checks the PDCCH in the immediate on-duration interval following the arrival of the  $Q_w$ -th packet. Consequently, the transmission of the first backlogged packet will be delayed an extra time denoted by  $T_w$  and we have

$$E[W_f] = \frac{Q_w - 1}{\lambda} + T_w, \quad (18)$$

with

$$E[W_f^2] = \sigma_{W_f}^2 + (E[W_f])^2 = \frac{Q_w - 1}{\lambda^2} + \left( \frac{Q_w - 1}{\lambda} + T_w \right)^2. \quad (19)$$

To compute this additional delay  $T_w$ , we may distinguish two different cases. First, if the  $Q_w$ -th packet (after entering the DRX mode) arrives during an on-duration period, downlink transmission can start at once and no extra delay is incurred. Conversely, if the  $Q_w$ -th packet arrives with DRX active and the UE is not listening to the PDCCH, a non-zero delay is added. Since Poisson arrivals are independently and uniformly distributed on any interval of time, we can assume that the arrival instant of the  $Q_w$ -th packet is uniformly distributed along the DRX cycle interval, which gets more true the higher the queue threshold or the inter-arrival times are, and hence an average extra delay of  $(T_s - T_{on})/2$  will be introduced with probability  $(T_s - T_{on})/T_s$ . Therefore, on average,  $T_w = (T_s - T_{on})^2/(2T_s)$ .

### C. The $\gamma$ Factor

The  $\gamma$  factor for Poisson traffic can be easily calculated just substituting the cumulative distribution function of the exponential distribution  $F_A(t) = 1 - e^{-\lambda t}$ ,  $t \geq 0$ , into (17):

$$\gamma = \frac{1 - \int_0^\infty (1 - e^{-\lambda t}) f_D(t) dt}{1 - \int_0^\infty (1 - e^{-\lambda(t+T_{in})}) f_D(t) dt} = e^{\lambda T_{in}}. \quad (20)$$

### D. Average Queueing Delay

Finally, substituting the results obtained for  $E[I]$  (and  $E[I^2]$ ) and  $E[W_f]$  (and  $E[W_f^2]$ ) into (14), the average queueing delay with Poisson traffic can be estimated as

$$E[W] = \frac{1 + \lambda^2 \sigma_s^2 + (1 - \rho)^2}{2\lambda(1 - \rho)} - \frac{Q_w - 1}{\lambda Q_w} + \frac{(Q_w + \lambda T_w)^2 - Q_w - 2(\lambda T_w + \gamma)}{2\lambda(Q_w + \lambda T_w + \gamma - 1)}, \quad (21)$$

with  $T_w = (T_s - T_{on})^2/(2T_s)$  and  $\gamma = e^{\lambda T_{in}}$ .

## VI. ADAPTIVE COALESCED DRX

A good tuning of the queue threshold is key for the performance of the coalesced DRX mechanism. If the queue threshold is too high, packets can get excessively delayed. On the contrary, setting a too low threshold reduces the power savings. An additional problem is that a single threshold value does not suit well for any possible incoming traffic. As shown

**Algorithm 1** Tuning algorithm of  $Q_w$  executed at the end of each coalescing cycle, just before entering the DRX mode.

---

**Require:** Estimates of the average delay in current cycle  $i$  ( $\widehat{W}[i]$ ) and the arrival rate ( $\widehat{\lambda}$ )  
 $Q_w[i+1] \leftarrow Q_w[i] + 2\widehat{\lambda}(W^* - \widehat{W}[i])$   
**if**  $Q_w[i+1] < 1$  **then**  
     $Q_w[i+1] \leftarrow 1$   
**else if**  $Q_w[i+1] > Q_{\max}$  **then**  
     $Q_w[i+1] \leftarrow Q_{\max}$   
**end if**

---

later, when the traffic load is low, increasing the threshold, even from modest values, produces unacceptable large increments on packet delay with only marginal increments on power savings. Under these circumstances, a low threshold is desirable, as it provides small latencies with good enough energy savings. For high traffic loads, the situation is just reversed. If the threshold were not increased, power savings would be greatly diminished.

In this section we present an algorithm to dynamically accommodate the  $Q_w$  parameter to incoming traffic. The main goal of our algorithm is to minimize power consumption in UEs while trying to maintain the average packet delay around a given target value  $W^*$ . So, to adjust the  $Q_w$  parameter to the existent traffic conditions, the average delay experienced by packets in a given coalescing cycle  $i$ , that is,  $\widehat{W}[i]$ , should be measured and compared with the target delay  $W^*$ . Then, if  $\widehat{W}[i] > W^*$ ,  $Q_w$  should be reduced to diminish packet delay. Conversely, if  $\widehat{W}[i] \leq W^*$ , current average packet delay is low enough and  $Q_w$  can be increased to reduce power consumption.

We know, therefore, the direction in which the queue threshold should be modified to make packet delay converge to the desired value, but we still have to select a proper function to update this parameter accurately. Intuitively, the more distant the measured average packet delay is from the target value, the more aggressive changes in the queue threshold should be. Therefore, we compute from (21) the partial derivative of  $E[W]$  with respect to  $Q_w$  to understand how this parameter affects average queueing delay in a given scenario:

$$\frac{\partial E[W]}{\partial Q_w} = \frac{1}{2\lambda} \left( 1 - \frac{2}{Q_w^2} + \frac{\lambda T_w - \gamma(\gamma + 1)}{(Q_w + \lambda T_w + \gamma - 1)^2} \right). \quad (22)$$

From this, it can be proved that  $\partial E[W]/\partial Q_w \leq (2\lambda)^{-1}$  for all  $Q_w \geq 1$  if  $\lambda \leq 4/T_w$  or  $\gamma \geq (\sqrt{4\lambda T_w - 7} - 1)/2$ , which holds true for usual DRX parameters. Consequently, we propose to modify  $Q_w$  using a conventional closed-loop controller with error signal  $W^* - \widehat{W}[i]$  and proportionality constant  $2\lambda$  to obtain a good compromise between  $Q_w$  stability and a fast response to changing traffic conditions, as shown in Algorithm 1. Also note that  $Q_w$  must not exceed a maximum value  $Q_{\max} = W_{\max}/S_{\max}$ , with  $S_{\max}$  being the maximum service time a packet could demand, to avoid introducing queueing delays greater than  $W_{\max}$ . The stability of this dynamic algorithm is evaluated in the Appendix.

To apply the proposed algorithm the eNB just needs to measure, for each connected UE, the average queueing delay in

each coalescing cycle and the arrival rate. As suggested in [25], we estimate the average arrival rate  $\widehat{\lambda}$  using the following exponential moving average:

$$\widehat{\lambda}_n = \left( 1 - e^{-A_n/k} \right) \frac{1}{A_n} + e^{-A_n/k} \widehat{\lambda}_{n-1}, \quad (23)$$

where  $A_n$  is the time between the arrivals of  $n+1$ -th and  $n$ -th packets and  $k = 2W_{\max}$ . A variable weight  $e^{-A_n/k}$  is used instead of a constant weight since, as stated in [25], this more closely reflects a fluid averaging process independent of the packetizing structure.

## VII. SIMULATION RESULTS

To evaluate the performance of the proposed scheme, we conducted several simulation experiments on an in-house simulator, available for download at [26]. As performance metrics, we select the power savings in the UE and the average queueing delay experienced by downlink traffic due to DRX operations. To estimate power savings, we measure the percentage of time spent by the UE in the low power mode, thus avoiding the reliance on any particular power consumption model.

Each simulation was run for 100 seconds and repeated ten times using different random seeds. Then, an average of the measured parameter was taken over all the runs. Although 95% confidence intervals have been also calculated, they will not be represented in the graphs since all of them are small enough and just clutter the figures.

In all the simulation experiments, the physical sub-frame (PSF) length is set to 1 ms. We assume that each packet transmission requires exactly one PSF.

### A. Coalesced DRX

To evaluate coalesced DRX and validate our model, we consider Poisson traffic with an increasing average arrival rate up to 0.9 packets per PSF. In this experiment, we used the following conventional DRX parameters:  $T_{\text{in}} = 10$  ms,  $T_s = T_{\text{off}} = 32$  ms and  $T_{\text{on}} = 2$  ms.<sup>3</sup>

Figure 4 shows the percentage of time spent in the low power mode and the average queueing delay with conventional DRX (i.e., without coalescing) and when coalescing is applied with three different queue thresholds ( $Q_w \in \{8, 32, 128\}$  packets). As expected, packet coalescing increases the time spent in the low power mode at the expense of increasing packet latency. Also note that our model produces very accurate predictions for the average queueing delay in all the simulated scenarios.

<sup>3</sup>The DRX cycle length has been selected to obtain a good trade-off between power efficiency and getting packet delays close to the target delay. Note that, with excessively short DRX cycles, the UE would check PDCCH too many times before reaching the queue threshold causing, therefore, an unnecessary high number of transitions between the DRX and the active mode that would increase power consumption. On the contrary, if DRX cycles were excessively long, the queue threshold could be reached well before the UE resumes listening to the PDCCH. This would prevent our adaptive proposal from achieving a good approximation to the target delay since the queue threshold could be only adjusted in a coarse-grained manner. We have checked through simulation that values between 16–64 ms for the DRX cycle length are suitable.

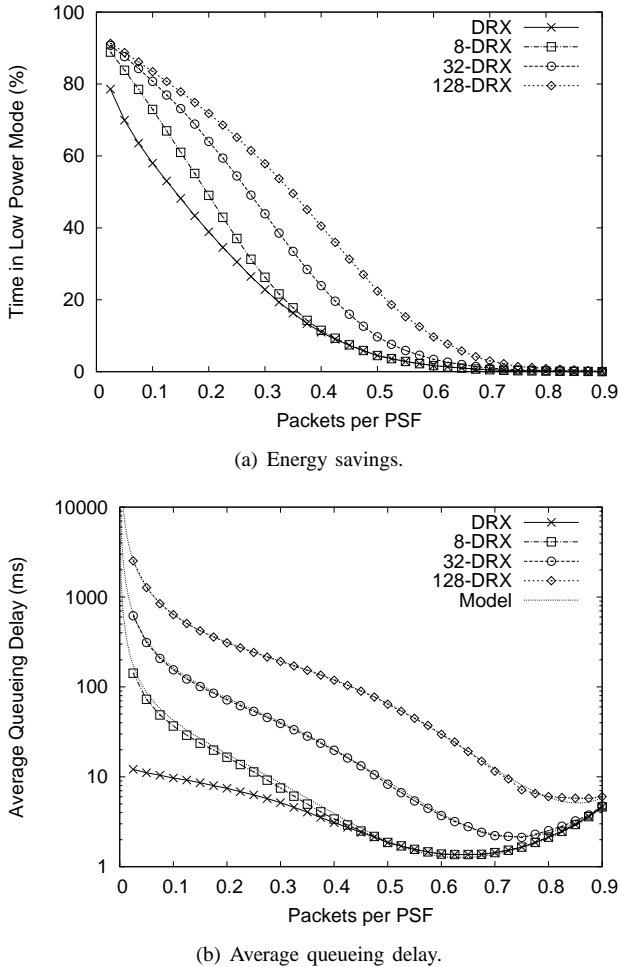


Fig. 4. Results with coalesced DRX.

Obviously, the higher the queue threshold is, the greater energy savings are obtained but, at low rates, using a high  $Q_w$  leads to unacceptable large increments on packet delay to just achieve marginal increments in power savings. Therefore, when traffic load is low, a low queue threshold should be used to improve energy savings while maintaining tolerable packet delays. On the contrary, a high queue threshold should be used at high rates to obtain significant energy savings. These results demonstrate that a single queue threshold value does not suit well for every downlink traffic stream, so an algorithm that dynamically adjusts this parameter in accordance with existing traffic conditions should be applied.

### B. Adaptive Coalesced DRX

We now evaluate our adaptive mechanism using the same DRX parameters as in the previous set of experiments. We configured our scheme with two different target average delays. If the UE were running some delay tolerant applications, the target delay could be configured with a high value, so we have firstly conducted several simulation experiments with  $W^* = 512$  ms. On the contrary, in a scenario with delay sensitive traffic, a low value should be assigned to the target delay, so we have also conducted some simulations with

$W^* = 64$  ms to evaluate our scheme under these more stringent conditions. Finally, we set  $W_{\max} = 2W^*$  in both scenarios.

Figure 5 shows the percentage of time spent in the low power mode and the average queueing delay obtained with conventional DRX and our adaptive coalesced DRX scheme. As expected, the adaptive mechanism is able to accommodate the queue threshold to the traffic load thus achieving significant energy savings while maintaining, at the same time, the average queueing delay around (or below) the configured target value. Obviously, the higher  $W^*$ , the greater energy savings with larger packet delays we obtained.

Figure 5(c) shows that our scheme adjusts the queue threshold to traffic conditions just choosing higher queue thresholds as traffic load increases. These higher thresholds enable greater power savings without sacrificing packet delay, since the time required to reach them is lower as packet inter-arrival times decrease. However, note that, at the highest loads, the average queue threshold stops increasing and maintains an almost constant value. This is a consequence of setting a maximum queue threshold  $Q_{\max}$  to bound the maximum queueing delay. This also explains why, in Fig. 5(b), the average queueing delay does not reach the predefined target at high loads.

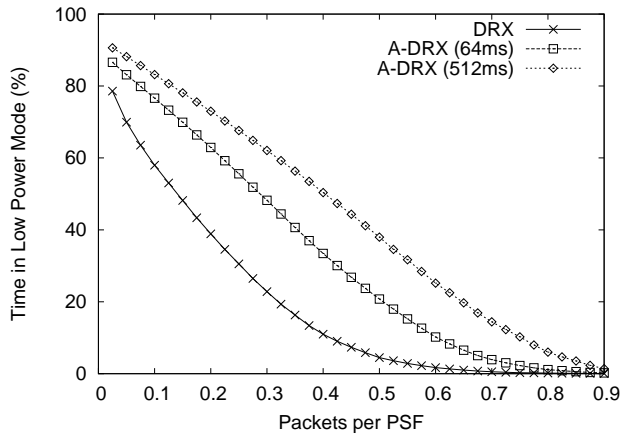
### C. Adaptive Coalesced DRX in Dynamic Scenarios

In all the previous experiments we simulated static scenarios with constant arrival rates. With the goal of exploring the speed of convergence of our algorithm, in the next experiment we simulate for 100 seconds a dynamic scenario in which the arrival rate is updated every 20 seconds following a pattern of  $\{0.1, 0.2, 0.4, 0.2, 0.1\}$  packets per PSF.

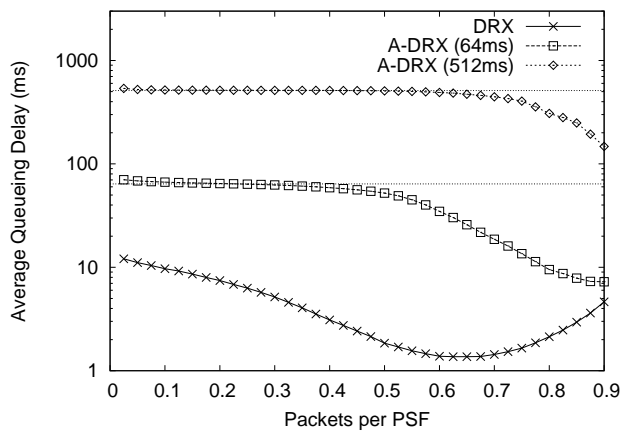
Figure 6(a) shows a representative example of the evolution of the queue threshold throughout the simulation for both  $W^*$ . It can be easily seen how our algorithm is able to quickly adjust the queue threshold to changing traffic conditions. Also note that the higher  $W^*$  value causes less variations in the queue threshold since it entails greater queue thresholds and, therefore, longer coalescing cycles. In Fig. 6(b) and 6(c) we show the energy savings and the average queueing delay obtained in each interval of 20 seconds respectively. We also show the average over the whole simulated time in the last cluster of data. As expected, our scheme maintains the average queueing delay around the target value in all the defined intervals and, therefore, the time spent in the low power mode is significantly increased.

### D. Adaptive Coalesced DRX with Self-Similar Traffic

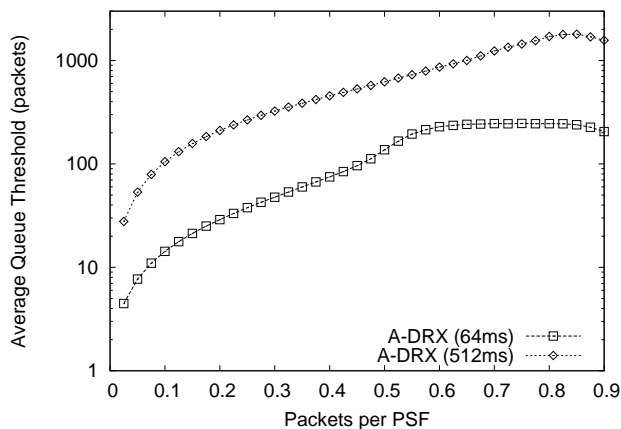
We have conducted some extra simulations to test our proposal under more realistic conditions. For instance, to characterize self-similar Internet traffic [27], in the following experiments we consider Pareto traffic with shape parameter  $\alpha = 1.5$ . The results obtained with Pareto traffic are shown in Fig. 7. As in the previous experiments, our proposal can achieve greater energy savings than standard DRX while maintaining the average queueing delay bounded at the same time. However, note that our scheme is now able to keep the average queueing delay closer to the target value even



(a) Energy savings.



(b) Average queueing delay.



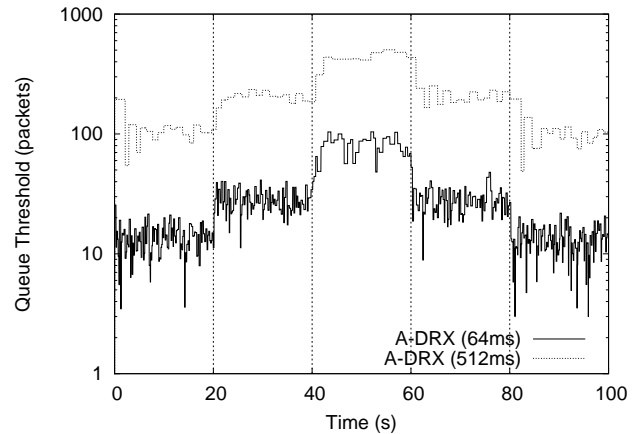
(c) Average queue threshold.

Fig. 5. Results with adaptive coalesced DRX.

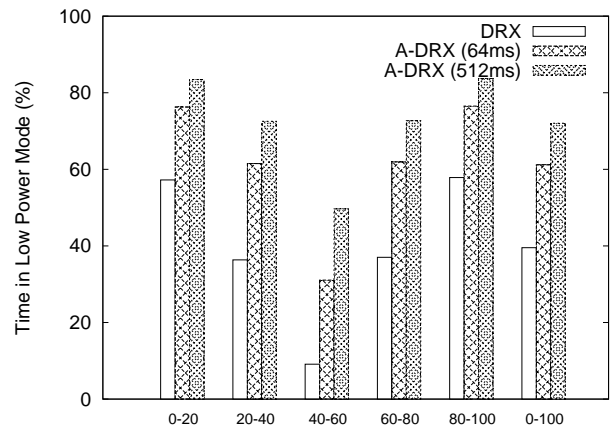
for the highest rates since Pareto traffic requires lower queue thresholds than Poisson traffic.

#### E. Adaptive Coalesced DRX with Video Streaming Traffic

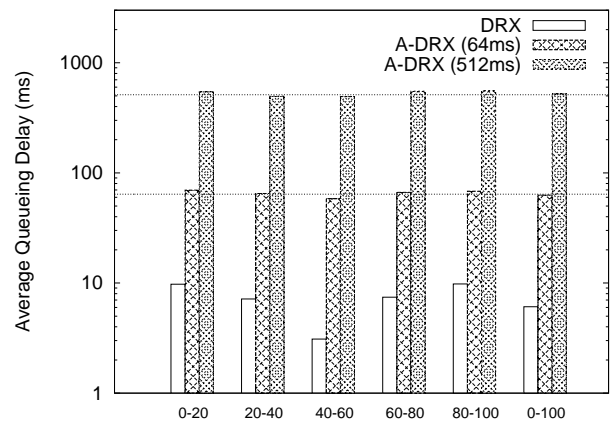
In recent years, mobile networks have experienced a huge increase in data traffic mainly due to video streaming services. In fact, it is expected that this trend continues in the next few years and Internet video services grow to account for more



(a) Queue threshold.



(b) Energy savings.

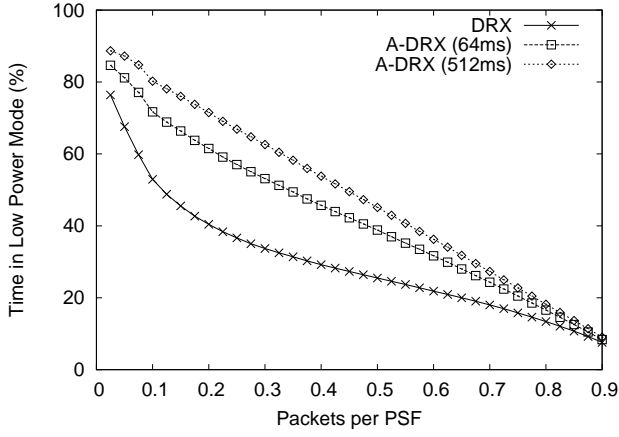


(c) Average queueing delay.

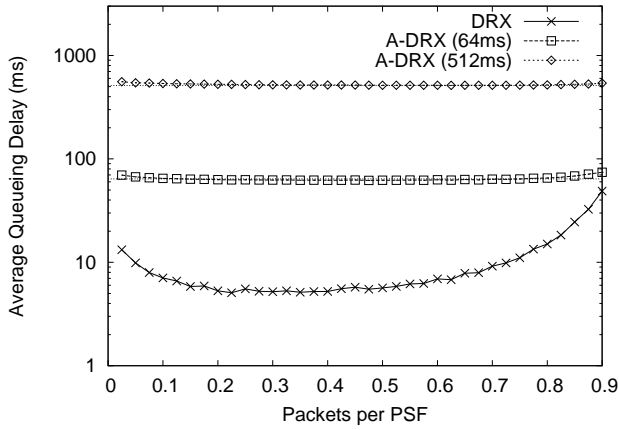
Fig. 6. Results in the dynamic scenario.

than 50% of mobile data traffic in 2019 (up from around 40% today) [28].

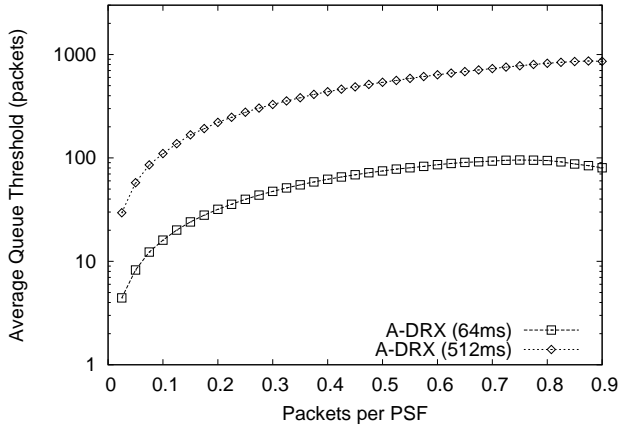
To assure that our proposal remains valid with this important traffic class, we fed the simulator with some traces from real video streaming applications previously used in [29], [30]. Traces from two different applications have been examined: YouTube, which uses HTTP streaming, and SopCast, which is a popular peer-to-peer (P2P) live streaming application [31].



(a) Energy savings.



(b) Average queueing delay.

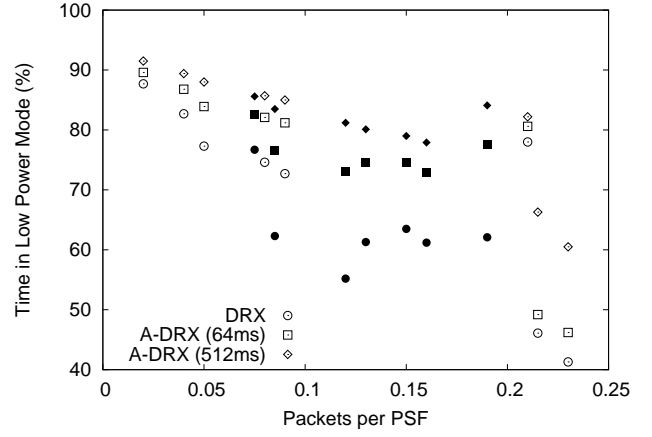


(c) Average queue threshold.

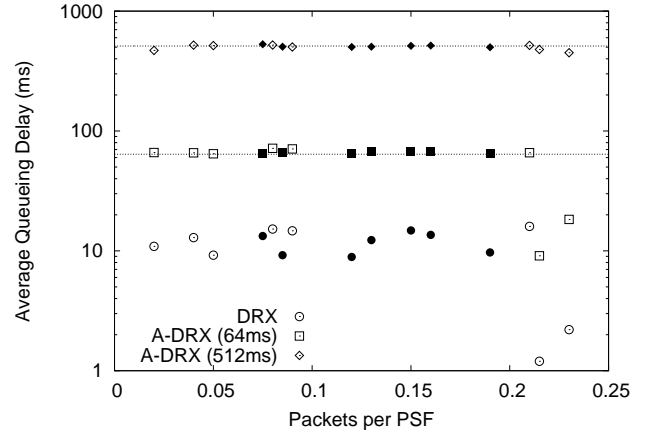
Fig. 7. Results with Pareto traffic.

SopCast uses a proprietary P2P streaming protocol to transmit the video content via UDP. The traces were collected using their respective native Android apps from several phones and tablets over different mobile networks.

Figure 8 shows some representative results obtained using these real traffic traces. As in the previous experiments with simulated traffic, our proposal is able to achieve notable improvements on energy savings, especially with the SopCast



(a) Energy savings.



(b) Average queueing delay.

Fig. 8. Results with video streaming traces. YouTube results are shown with unfilled points while filled points are used to show the results with SopCast.

application, while keeping the average queueing delay close to the target value.

## VIII. DISCUSSION AND RELATED WORK

Unlike most DRX schemes proposed to improve energy efficiency of UEs [3], [6], [7], [8], [9], [10], [11], [12], [13], the technique discussed in this paper does not require DRX reconfiguration and, therefore, does not increase RRC signaling overhead. Notice that an excess of signaling overhead has a non-negligible cost on energy efficiency since it adds considerable processing load to UEs and to other networking components [32]. Additionally, these schemes require to solve a relatively complex optimization problem each time the traffic conditions at any UE change, thus increasing significantly the processing load of the eNB. Our proposal, on the contrary, just requires a few simple computations per UE to be done.

To the best of our knowledge, CDA-DRX is the only proposal able to reduce energy consumption without introducing extra signaling overhead [33]. CDA-DRX allows UEs to autonomously adjust their DRX cycles according to ongoing user activity by using two synchronized counters in both the UE and the eNB. One of these counters keeps account of the number of consecutive active DRX periods while the other one

counts consecutive idle DRX periods. Two trigger thresholds, one for each of these counters, are also defined so that, when each counter reaches its corresponding threshold, the length of the DRX cycle is extended (or reduced) simultaneously in both the UE and the eNB without the need of DRX reconfiguration. Unfortunately, this scheme requires modifying the 3GPP RRC protocol [4] to permit UEs to indicate to the eNB whether they support CDA-DRX and, if so, to negotiate between them the involved CDA-DRX parameters (that is, the trigger thresholds and the series of DRX cycle lengths supported). On the contrary, our scheme only requires some minor changes to eNB operations, so existing wireless protocols can still be used without any modification at all.

Finally, we would like to highlight that our scheme just requires the configuration of two straightforward parameters: the average and the maximum delay desired for downlink traffic at the eNB. These parameters could be configured taking into account the power preference indication (PPI) sent by the UE through the UE assistance information RRC message [4]. If the UE is running delay tolerant applications, it will send the PPI bit active and, then, the eNB could select high values for the target delays. Conversely, with delay sensitive traffic, the PPI bit will be set to zero and the eNB should select lower values for them.<sup>4</sup> Maximum target delays around 50–100 ms for delay sensitive applications and around 300 ms for delay tolerant applications are suitable [34]. If the UE traffic is composed of several flows with different degrees of delay sensitivity, the target delay should be configured with a value suitable to the most stringent flow and the eNB should schedule the transmission of UE packets according to their delay requirements [22].

## IX. CONCLUSIONS

This paper presents a promising DRX scheme able to improve energy efficiency of UEs while maintaining the average packet delay bounded at the same time. Essentially, we propose that eNBs delay downlink transmission until their downstream queues reach a threshold, thus increasing the amount of time the UEs spend in DRX mode. Since a single value for this threshold does not suit well for all possible traffic loads, we have also presented an adaptive algorithm able to adjust the queue threshold in accordance with existing traffic conditions.

Unlike other power saving schemes proposed in the literature, our mechanism does not increase RRC signaling overhead since it does not rely on DRX reconfiguration. Furthermore, it can be easily deployed in LTE/LTE-A networks since it is very simple to configure and does not require any changes to the wireless protocols in operation at the current time.

<sup>4</sup>For those earlier systems to 3GPP Release 11 that lack a way to communicate their power preferences to the network, the eNB could configure coalesced DRX parameters without UE assistance trying, for example, some deep packet inspection to guess running applications and their corresponding delay requirements. Obviously, this approach requires adding quite extra overhead at the eNBs, so, when possible, the use of the PPI bit to communicate UE preferences to the eNB should be preferred.

## ACKNOWLEDGMENTS

The authors thank Dr. Mohammad Ashrafu Hoque from the University of Helsinki for kindly providing us with some of the traffic traces employed in [29]. Traces used in [30] were obtained from the UMass Trace Repository [35].

Work supported by the European Regional Development Fund (ERDF) and the Galician Regional Government under agreement for funding the Atlantic Research Center for Information and Communication Technologies (AtlantTIC).

## APPENDIX STABILITY ANALYSIS

The adaptive  $Q_w$  tuning scheme proposed in Algorithm 1 can be modeled as the following dynamical system:

$$Q_w[i+1] = \min \{ \max \{ Q_w[i] + 2\lambda(W^* - f(Q_w[i])), 1 \}, Q_{\max} \} \quad (24)$$

in the discrete-time index  $i = 1, 2, \dots$ , where  $f(\cdot)$  captures the dependence of the average queueing delay on the queue threshold. Since  $f(\cdot)$  is a continuous, increasing and differentiable function of  $Q_w$  with bounded derivative, this system clearly reaches the fixed equilibrium point  $Q_w^*$  when  $f(Q_w^*) = W^*$ . Then, assuming  $1 \leq Q_w^* \leq Q_{\max}$  since, otherwise, the target delay  $W^*$  is not achievable, (24) can be written as

$$Q_w[i+1] = Q_w[i] + 2\lambda(W^* - f(Q_w[i])). \quad (25)$$

It is straightforward to prove via linearization that this system is stable if the derivative of (25) at the equilibrium point has an absolute value strictly less than one, that is,

$$|1 - 2\lambda f'(Q_w^*)| < 1. \quad (26)$$

Therefore, the stability condition is met if  $0 < f'(Q_w^*) < 1/\lambda$ . From (22), the condition  $f'(Q_w^*) < 1/\lambda$  holds if and only if

$$\frac{\lambda T_w - \gamma(\gamma + 1)}{(Q_w^* + \lambda T_w + \gamma - 1)^2} - \frac{2}{Q_w^{*2}} < 1, \quad (27)$$

what is true for all  $\lambda$  and  $Q_w^* \geq 1$  since  $\gamma \geq 1$  as proved in Section IV-B. On the other hand, the condition  $f'(Q_w^*) > 0$  holds if and only if

$$\frac{2}{Q_w^{*2}} - \frac{\lambda T_w - \gamma(\gamma + 1)}{(Q_w^* + \lambda T_w + \gamma - 1)^2} < 1. \quad (28)$$

To check this condition, we must consider two different cases. If  $\lambda T_w - \gamma(\gamma + 1) \geq 0$ , that is,  $\lambda \geq \gamma(\gamma + 1)/T_w$ , (28) is true for all  $Q_w^* > \sqrt{2}$ . Clearly, this condition is fulfilled in almost all reasonable scenarios since it is highly probable that the equilibrium point surpasses  $\sqrt{2}$  under the previous assumption of high arrival rates. Unfortunately,  $\lambda T_w - \gamma(\gamma + 1) < 0$  with usual DRX parameters. In this case, the LHS of (28) goes to zero when  $Q_w^* \rightarrow \infty$ , so there must exist a value  $q$  of the queue threshold such that (28) holds for any  $Q_w^* > q$  guaranteeing system stability. Usually, the  $Q_w^*$  required to achieve a given target delay  $W^*$  is high enough to fulfill (28). This is the case for all the simulated scenarios. However, if  $W^*$  is too stringent,  $Q_w^*$  may be smaller than  $q$  at the lowest rates, so, in those rare scenarios with excessively low target delays, the stability of the algorithm could not be guaranteed.

## REFERENCES

- [1] 3GPP TS 36.300, "LTE; Evolved Universal Terrestrial Radio Access (E-UTRA) and Evolved Universal Terrestrial Radio Access Network (E-UTRAN); Overall description," ETSI, Mar. 2014, Rel. 11, v. 11.9.0.
- [2] 3GPP TS 36.321, "LTE; Evolved Universal Terrestrial Radio Access (E-UTRA); Medium Access Control (MAC) protocol specification," ETSI, Mar. 2014, Rel. 11, v. 11.5.0.
- [3] C. S. Bontu and E. Illidge, "DRX mechanism for power saving in LTE," *IEEE Commun. Mag.*, vol. 47, no. 6, pp. 48–55, Jun. 2009.
- [4] 3GPP TS 36.331, "LTE; Evolved Universal Terrestrial Radio Access (E-UTRA); Radio Resource Control (RRC); Protocol specification," ETSI, Mar. 2015, Rel. 11, v. 11.11.0.
- [5] S. Fowler, R. S. Bhamber, and A. Mellouk, "Analysis of adjustable and fixed DRX mechanism for power saving in LTE/LTE-Advanced," in *IEEE International Conference on Communications (ICC)*, Jun. 2012, pp. 1964–1969.
- [6] R. M. Karthik and A. Chakrapani, "Practical algorithm for power efficient DRX configuration in next generation mobiles," in *IEEE INFOCOM*, Apr. 2013, pp. 1106–1114.
- [7] A. T. Koc, S. C. Jha, R. Vannithamby, and M. Torlak, "Device power saving and latency optimization in LTE-A networks through DRX configuration," *IEEE Trans. Wireless Commun.*, vol. 13, no. 5, pp. 2614–2625, May 2014.
- [8] Y. Wen, J. Liang, K. Niu, and W. Xu, "Performance analysis and optimization of DRX mechanism in LTE," in *3rd IEEE International Conference on Network Infrastructure and Digital Content (IC-NIDC)*, Sep. 2012, pp. 71–75.
- [9] Y.-P. Yu and K.-T. Feng, "Traffic-based DRX cycles adjustment scheme for 3GPP LTE systems," in *IEEE Vehicular Technology Conference (VTC Spring)*, May 2012, pp. 1–5.
- [10] S. Alouf, V. Mancuso, and N. C. Fofack, "Analysis of power saving and its impact on web traffic in cellular networks with continuous connectivity," *Pervasive and Mobile Computing*, vol. 8, no. 5, pp. 646–661, Oct. 2012.
- [11] K. Wang, X. Li, and H. Ji, "Modeling 3GPP LTE Advanced DRX mechanism under multimedia traffic," *IEEE Commun. Lett.*, vol. 18, no. 7, pp. 1238–1241, Jul. 2014.
- [12] K. Wang, S. Chen, X. Li, and H. Ji, "DRX-aware transmission policy for time varying channels with delay constraint," in *IEEE International Conference on Communications (ICC)*, Jun. 2014, pp. 2381–2387.
- [13] C.-C. Tseng, H.-C. Wang, F.-C. Kuo, K.-C. Ting, H.-H. Chen, and G.-Y. Chen, "Delay and power consumption in LTE/LTE-A DRX mechanism with mixed short and long cycles," *IEEE Trans. Veh. Technol.*, vol. In press, 2015.
- [14] 3GPP TR 25.913, "UMTS; LTE; Requirements for Evolved UTRA (E-UTRA) and Evolved UTRAN (E-UTRAN)," ETSI, Dec. 2009, Rel. 9, v. 9.0.0.
- [15] K. Christensen, P. Reviriego, B. Nordman, M. Bennett, M. Mostowfi, and J. A. Maestro, "IEEE 802.3az: the road to energy efficient ethernet," *IEEE Commun. Mag.*, vol. 48, no. 11, pp. 50–56, Nov. 2010.
- [16] S. Herrería-Alonso, M. Rodríguez-Pérez, M. Fernández-Veiga, and C. López-García, "A GI/G/1 model for 10 Gb/s energy efficient ethernet links," *IEEE Trans. Commun.*, vol. 60, no. 11, pp. 3386–3395, Nov. 2012.
- [17] M. Rodríguez-Pérez, S. Herrería-Alonso, M. Fernández-Veiga, and C. López-García, "Improving energy efficiency in upstream EPON channels by packet coalescing," *IEEE Trans. Commun.*, vol. 60, no. 4, pp. 929–932, Apr. 2012.
- [18] S. Herrería-Alonso, M. Rodríguez-Pérez, M. Fernández-Veiga, and C. López-García, "On the use of the doze mode to reduce power consumption in EPON systems," *J. Lightw. Technol.*, vol. 32, no. 2, pp. 285–292, Jan. 2014.
- [19] M. Gupta, S. C. Jha, A. T. Koc, and R. Vannithamby, "Energy impact of emerging mobile internet applications on LTE networks: Issues and solutions," *IEEE Commun. Mag.*, vol. 51, no. 2, pp. 90–97, Feb. 2013.
- [20] J. G. Andrews, "Seven ways that HetNets are a cellular paradigm shift," *IEEE Commun. Mag.*, vol. 51, no. 3, pp. 136–144, Mar. 2013.
- [21] H. Bo, T. Hui, C. Lan, and Z. Jianchi, "DRX-Aware scheduling method for delay-sensitive traffic," *IEEE Commun. Lett.*, vol. 14, no. 12, pp. 1113–1115, Dec. 2010.
- [22] J.-M. Liang, J.-J. Chen, H.-H. Cheng, and Y.-C. Tseng, "An energy-efficient sleep scheduling with QoS consideration in 3GPP LTE-Advanced networks for internet of things," *IEEE J. Emerging and Sel. Topics Circuits Syst.*, vol. 3, no. 1, pp. 13–22, Mar. 2013.
- [23] K. T. Marshall, "Bounds for some generalizations of the GI/G/1 queue," *Operations Research*, vol. 16, no. 4, pp. 841–848, Jul. 1968.
- [24] D. P. Heyman and K. T. Marshall, "Bounds on the optimal operating policy for a class of single-server queues," *Operations Research*, vol. 16, no. 6, pp. 1138–1146, Nov. 1968.
- [25] I. Stoica, S. Shenker, and H. Zhang, "Core-stateless fair queueing: A scalable architecture to approximate fair bandwidth allocations in high-speed networks," *IEEE/ACM Trans. Netw.*, vol. 11, no. 1, pp. 33–46, Feb. 2003.
- [26] S. Herrería-Alonso, "LteSimulator: a Java simulator for LTE traffic," Feb. 2015. [Online]. Available: <https://github.com/sherreria/LteSimulator>
- [27] M. E. Crovella and A. Bestavros, "Self-similarity in world wide web traffic: evidence and possible causes," *IEEE/ACM Trans. Netw.*, vol. 5, no. 6, pp. 835–846, Dec. 1997.
- [28] Ericsson, "Mobility report," Jun. 2014. [Online]. Available: <http://www.ericsson.com/res/docs/2014/ericsson-mobility-report-june-2014.pdf>
- [29] M. A. Hoque, M. Siekkinen, J. K. Nurminen, M. Aalto, and S. Tarkoma, "Mobile multimedia streaming techniques: QoE and energy saving perspective," *Pervasive and Mobile Computing*, vol. 16, no. A, pp. 96–114, Jan. 2015.
- [30] P. M. Eittenberger, M. Hamatschek, M. Grossmann, and U. R. Krieger, "Monitoring mobile video delivery to android devices," in *Proceedings of the 4th ACM Multimedia Systems Conference*, ser. MMSys '13, 2013, pp. 119–124.
- [31] "Sopcast." [Online]. Available: <http://www.sopcast.org/>
- [32] P. K. Gupta, R. V. Rajakumar, C. S. Kumar, and G. Das, "Analytical evaluation of signalling cost on power saving mechanism in mobile networks," in *IEEE TENCN Spring Conference*, Apr. 2013, pp. 376–380.
- [33] E. Liu, J. Zhang, and W. Ren, "Adaptive and autonomous power-saving scheme for beyond 3G user equipment," *IET Communications*, vol. 7, no. 7, pp. 602–610, May 2013.
- [34] 3GPP TS 23.203, "Policy and charging control architecture," ETSI, Dec. 2014, Rel. 13, v. 13.2.0.
- [35] "UMass Trace Repository. ACM MMSys conference dataset archive." [Online]. Available: <http://traces.cs.umass.edu/index.php/Mmsys/Mmsys>